Research Square

Preprints are preliminary reports that have not undergone peer review.
They should not be considered conclusive, used to inform clinical practice,
or referenced by the media as validated information.

High-Strength Binderless Material from Brewer's Spent Grain through NaOH Pretreatment

Sungwoo Park

spark22@cau.ac.kr

Chung-Ang University

Seongjong Kim

Chung-Ang University

Choongwan Koo

Incheon National University

Yang-Ju Son

Chung-Ang University

Article

Keywords: Brewer's Spent Grains (BSG), Natural lignocellulosic fibers, Alkali pretreatment, Hot pressing, In situ consolidation, Self-bonding behavior

Posted Date: November 12th, 2026

DOI: https://doi.org/10.21203/rs.3.rs-11474280/v1

License: This work is licensed under a Creative Commons Attribution 4.0 International License.
Read Full License

Additional Declarations: No competing interests reported.

High-Strength Binderless Material from Brewer's Spent Grain through NaOH Pretreatment

Sungwoo Park[a,b,1,*] Seongjong Kim[a], Choongwan Koo[c], Yang-Ju Son[d]

[a] *School of Architecture & Building Science, Chung-Ang University, 84 Heukseok-ro, Dongjak-gu, Seoul 06974, Republic of Korea*
[b] *Department of Smart Cities, Chung-Ang University, 84 Heukseok-ro, Dongjak-gu, Seoul 06974, Republic of Korea*
[c] *Division ofArchitecture & Urban Design, Incheon National University, Incheon, Republic of Korea*
[d] *Department of Food and Nutrition, Chung-Ang University, Anseong 17546, Republic of Korea*

Abstract

Brewer's spent grain (BSG) is a lignocellulosic brewing by-product with other nutrient components. Although BSG-only particleboards have previously been produced by hot pressing, the effects of alkali pretreatment on consolidation and expansion during pressing remain insufficiently characterized. Raw and NaOH-treated BSG were hot-pressed without added adhesives, and specimen-height changes were monitored in situ using a laser displacement sensor. Pressing temperature, duration, and pressure were examined alongside chemical composition, thermal behavior, microstructure, and mechanical properties. Raw BSG showed expansion and loss of integrity at elevated pressing temperatures, whereas NaOH treatment followed by washing enabled stable consolidation at temperatures up to 180 °C. Treatment reduced the measured hemicellulose and lignin fractions, while subsequent washing reduced protein and lipid contents. The highest compressive strength reached 71.3 MPa, approximately 32% above the maximum measured for raw BSG. These results identify pretreatment-

* Corresponding author.
Email address: spark22@cau.ac.kr (S. Park)

dependent consolidation behavior as an important factor in processing BSG into high-strength binderless composites.

Keywords: Brewer's Spent Grains (BSG), Natural lignocellulosic fibers, Alkali pretreatment, Hot pressing, In situ consolidation, Self-bonding behavior

1. Introduction

Food waste upcycling is an emerging research area from a sustainability perspective. Food waste is continuously generated during food processing and consumption, ultimately originating from natural resources. Upcycling food waste yields two significant benefits: reducing waste disposal volumes and adding value to the waste, thereby contributing to a circular economy. Recently, the European Commission introduced the Circular Economy Action Plan as part of the Green Deal strategy, highlighting a paradigm shift in industrial production [1]. Consequently, research on food-waste upcycling has become increasingly important.

The brewing industry generates substantial food waste, primarily in the form of brewers' spent grains (BSG). BSG is the major solid by-product of the brewing process, accounting for up to 85% of breweries' total solid waste [2]. With global beer production generating approximately 40 million tons of BSG annually [3], developing alternative strategies for BSG disposal and valorization has become a critical research topic [4]. BSG is rich in proteins, lipids, and dietary fibers—including lignin, cellulose, and hemicellulose [5-7]—and has been considered as animal feed [8,9]. However, BSG rapidly deteriorates within 2 days due to its high moisture content (>80%) [4, 10], even at approximately 5 °C [10]. Additionally, increasingly stringent regulations on the quality of animal feed necessitate the development of alternative and sustainable disposal methods for BSG [11].

The potential use of BSG as a component in various building materials has been investigated. Incorporating BSG in bricks has been shown to improve the permeability and

thermal insulation properties. However, the BSG content is typically limited to 5 wt%, as higher proportions lead to a deterioration in the compressive and flexural strengths of the bricks [12,13].

BSG has also been explored as a partial substitute for wood particles in wood-based particleboards, owing to its fibrous composition rich in lignin and cellulose, which resembles the components of wood [14]. Nevertheless, increasing the BSG content beyond approximately 10% tends to impair the mechanical properties, particularly the compressive and flexural strengths of the composite boards [15,16]. This reduction is primarily attributed to the disruption of bonding between wood particles and adhesives caused by the presence of BSG fibers [15]. Furthermore, the smaller size and lower rigidity of BSG fibers compared to wood fibers contribute to the observed reduction in strength [17].

An additional approach introduced in a previous study involved combining BSG with flour, jaggery, and xanthan gum to develop bio-based, moldable materials as potential substitutes for plastics. However, the maximum BSG content remained limited to 10 wt% due to mechanical constraints [18]. These limitations highlight a recurring challenge: despite innovative applications, the incorporation of BSG into conventional building materials is generally limited to 5–10 wt%, with these approaches relying on additional binding materials rather than utilizing the self-bonding potential of BSG.

Thermal compression can promote self-bonding between lignocellulosic particles of BSG. During thermal compression, fibers such as lignin, hemicellulose, and cellulose undergo chemical and physical reactions [19]. Under high temperatures, inter-fiber bonds break, causing the material to transition into a plastic state [20,21]. Subsequently, fibers are physically condensed with pressure, resulting in cross-linked polymer structures through dehydration, hydrolysis, and oxidation [22-24]. Thus, heat and pressure are critical to the self-bonding behavior observed in the hot pressing of natural fibers [25]. This mechanism has been leveraged to develop binderless

fiberboards from natural sources such as rice straw, wheat straw, oil palm, coconut, bagasse, and kenaf fiber [26-30].

A previous study demonstrated the feasibility of producing binderless particleboards entirely from brewer's spent grain (BSG) through hot pressing; however, the investigation primarily focused on the effects of particle size and pressing temperature on the resulting board properties [31]. Despite this progress, the influence of BSG composition on consolidation behavior during hot pressing and the resulting mechanical performance remains insufficiently understood. We hypothesized that removing non-fibrous components, particularly proteins and lipids, could improve the consolidation behavior and mechanical properties of BSG-based composites. To demonstrate this hypothesis, alkaline pretreatment using a NaOH solution was applied.

This study aimed to investigate the effects of NaOH pretreatment and subsequent washing on the hot-pressing behavior and mechanical performance of binderless composites made entirely from BSG. First, the effects of pressing temperature, duration, and pressure on the compressive strength of untreated BSG composites were evaluated. In situ changes in specimen height were monitored using a laser displacement sensor to characterize consolidation and expansion during hot pressing. Subsequently, changes in chemical composition, thermal behavior, and microstructure induced by NaOH pretreatment and washing were examined to understand their relationships with consolidation behavior and mechanical performance. By linking compositional changes to hot-pressing behavior and mechanical properties, this study provides insights into the role of alkaline pretreatment in improving the processability and performance of binderless BSG composites.

2. Materials and test methods

2.1. Raw materials and sample preparation

Approximately 80 kg of BSG was obtained immediately after beer production from a local brewery in Korea. The BSG was immediately transported to the laboratory and oven-dried at 85 °C until the weight change over a 30 min interval was less than 1%. The dried BSG was then homogenized in a rotary drum mixer, followed by 3 min of grinding using a mixer (HMF-4010SS, Hanil Electric Co. Ltd.). The particle-size distribution is shown in **Figure 1**. It should be noted that the NaOH-treated specimens exhibited similar particle size distributions.

The dried BSG was sealed in airtight containers to prevent moisture absorption prior to use. The chemical composition of the BSG is summarized in **Table 1**. Proximate analysis was conducted in accordance with methods established by the American Association of Cereal Chemists (AACC, 2000) [32]. Moisture, crude protein, crude lipid, and ash contents were analyzed following AACC Methods 44-15A, 46-13, 30-25, and 08-01, respectively. Carbohydrate content was determined by subtracting the sum of moisture, protein, lipid, and ash from 100%. The cellulose, hemicellulose, and lignin contents were determined according to the procedure described by Jung et al. [33]. Note that the total carbohydrate content exceeds the combined cellulose, hemicellulose, and lignin contents, suggesting the presence of other carbohydrate constituents, such as pectin, in BSG.

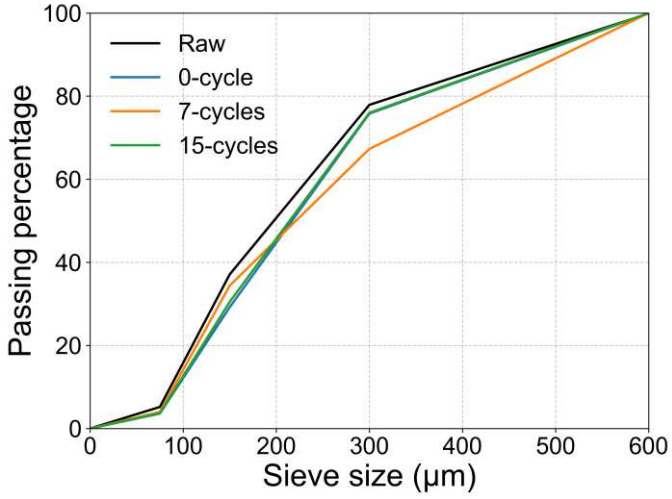


Figure 1. Sieve-based particle size distribution of the prepared BSG powder.

Table 1. Chemical composition of raw BSG.

Components	wt%±Standard deviation
Moisture	5.43 ± 0.09
Crude protein	15.26 ± 0.07
Crude lipid	6.20 ± 0.03
Ash	2.24 ± 0.04
Carbohydrate	70.86 ± 0.12
Cellulose	12.18 ± 0.06
Hemicellulose	22.78 ± 0.37
Lignin	13.16 ± 1.16

To remove non-fibrous organic components, such as proteins and lipids, the BSG was chemically pretreated with a sodium hydroxide (NaOH) solution. Commercial NaOH beads (98.0% purity) were dissolved in deionized water and allowed to cool to room temperature before use. A total of 100 g of dried BSG was immersed in 1 kg of 0.1 M NaOH solution and stirred continuously at 60 °C for 1 h, as described in a previous study [34].

Following the alkaline treatment, the BSG was removed from the solution and rinsed by immersion in 1 kg of deionized water with stirring for 5 min. This washing step was repeated 0, 7, and 15 times to remove residual NaOH and solubilized components. The treated BSG was then oven-dried at 85 °C for 24 h and subsequently ground to achieve a particle size distribution comparable to that of the raw BSG, as illustrated in **Figure 1**.

2.2. Hot pressing

The hot-pressing machine (QMESYS, QM900LA) and molds used in this study are illustrated in **Figure 2**. Two mold types were employed: a cylindrical mold with internal dimensions of 25 × 10 mm for compressive strength testing, and a prismatic (bar-shaped) mold with internal dimensions of 100 × 25 × 10 mm for flexural strength testing. 7 g and 10 g of BSG were used for the cylindrical and prismatic molds, respectively. These material quantities were determined based on preliminary studies to ensure consistent specimen formation.

Heating was provided by parallel top and bottom platens, which raised the mold temperature to the designated pressing temperature before loading. Once the target temperature

was reached, the BSG was placed into the cylindrical or prismatic mold, and the desired pressure was applied via an actuator-driven bottom platen that moved upward to compress the material for a specified duration while maintaining a constant temperature. In this study, the temperature maintained by the heating platens during pressing is referred to as the hot-pressing temperature. The system incorporated a feedback-controlled mechanism that continuously adjusted the applied pressure to compensate for specimen shrinkage during densification, thereby ensuring stable and uniform consolidation throughout the hot-pressing process.

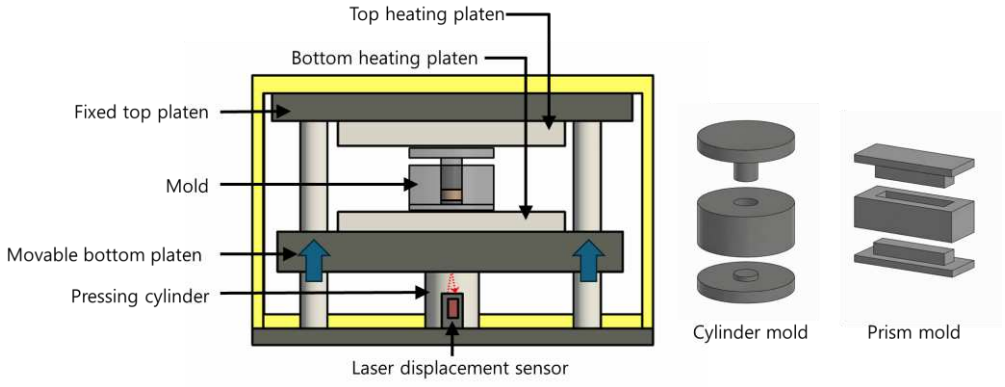


Figure 2. Schematic drawing of the hot-pressing machine and the molds used in this study.

During hot pressing, material consolidation was monitored using a laser displacement sensor (CD2H-130M12, OPTEX FA) to quantify the in situ change in specimen height. The sensor has a measurement range of 130 ± 70 mm and a resolution of 4 μm. A representative displacement profile of the specimens hot-pressed at 130 °C under 20 MPa pressure for 15 min is shown in **Figure 3**. The sensor continuously tracked the vertical displacement of the movable bottom platen throughout the pressing process.

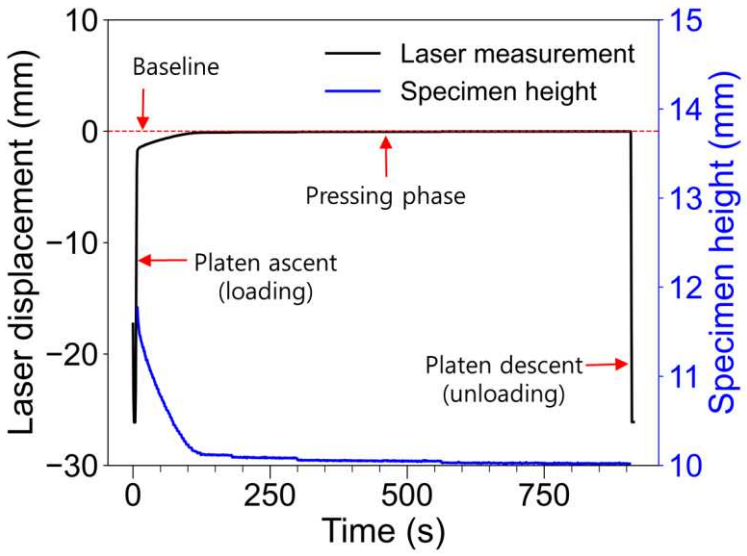


Figure 3. Example of in situ specimen height measurement during BSG binder formation, hot-pressed at 130 °C under 20 MPa pressure for 15 min using a laser displacement sensor.

The onset of pressing was visually identified from the displacement profile, and the pressing time was recorded from the moment the designated pressure was reached. Prior to hot pressing, a baseline displacement of 0 mm was established, corresponding to the fully closed mold configuration. At this point, the applied load is supported by the mold assembly rather than the BSG material; therefore, the initial BSG mass was carefully adjusted to ensure proper contact with the mold surfaces before meaningful load transfer occurred. After the pressing stage was completed, the platen was lowered. Using the baseline reference—at which the internal specimen height is 10 mm—the time-dependent changes in specimen height during the pressing were subsequently calculated.

After hot pressing, the specimens were demolded and stored in a sealed container at ambient conditions for 24 h before testing. This resting period was critical, as it significantly enhanced compressive strength compared to specimens tested immediately after pressing.

2.3. Characterization of the BSG and the BSG binder

TGA was performed to examine the structural changes in BSG induced by treatment with the NaOH solution. The measurements were conducted using a TGA 55 (TA Instruments™) from 30 to 900 °C at a constant heating rate of 10 °C/min under nitrogen.

Compressive strength was measured at a loading rate of 1 mm/min, and the reported value for each condition corresponds to the average of three cylindrical specimens (25 mm × 10 mm). Statistical differences in compressive strength were evaluated using one-sided Welch's t-tests, which do not assume equal variances between groups. Directional hypotheses were defined a priori: NaOH treatment was expected to increase strength, whereas increasing the number of washing cycles was expected to decrease strength. Comparisons involving failed binder formation were excluded because no measurable strength data were available. Statistical significance was accepted at $p < 0.05$.

Flexural strength was evaluated as the modulus of rupture (MOR) using a three-point bending test, with each value representing the mean of three prismatic specimens (100 mm × 20 mm × 3.3 mm).

Changes in the BSG fibers induced by NaOH treatment were examined using SEM (SIGMA 360, Carl Zeiss, Germany). Small particles were collected, mounted, and sputter-coated with platinum before analysis. SEM observations were conducted at an accelerating voltage of 5 kV. For microstructures of the BSG binders, thin sections approximately 0.3 mm thick were prepared and examined using scanning electron microscopy (Carl Zeiss Sigma 360) and optical microscopy (Carl Zeiss Axio Zoom V16).

3. Results and discussions

3.1. Effect of hot-pressing parameters on the compressive strength

This study sequentially investigated the effects of hot-pressing temperature, duration, and pressure on the compressive strength of the BSG binder. The optimal value identified at each stage was fixed for the subsequent evaluation.

The hot-pressing temperature plays a crucial role in determining the compressive strength of BGS binders. **Figure 4a** shows the compressive strength of the BGS specimens pressed at 20 MPa. Missing data correspond to processing conditions under which binder formation failed. The maximum compressive strength increased significantly with temperature, rising from 12.5 MPa at 100 °C to 54.5 MPa at 130 °C. This enhancement is likely attributed to improved consolidation and bonding within the binder matrix at elevated temperatures, which will be discussed in detail. However, further increasing the temperature to 140°C resulted in a sharp decline in strength to approximately 19 MPa, accompanied by visible cracking in the specimens. This suggests that thermal degradation of the organic components in the BSG compromises structural integrity. Based on this trend, 120-130 °C is identified as the optimal pressing temperature for maximizing compressive strength without inducing thermal damage.

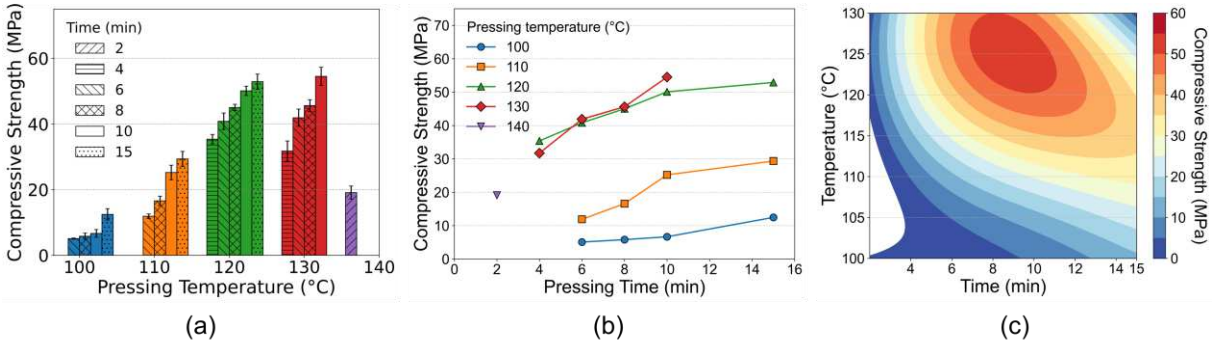


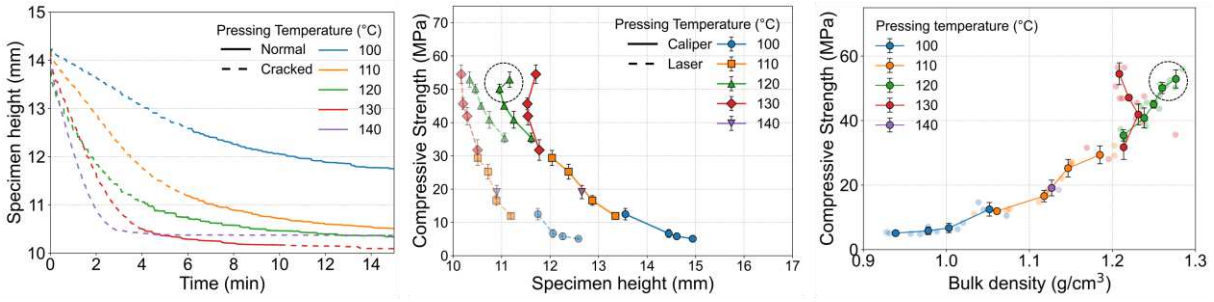
Figure 4. Compressive strength of BSG binders hot-pressed under a constant pressure at 20 MPa: (a) compressive strength at varying temperatures with different pressing times, (b) strength development over time at different temperatures, and (c) support vector regression analysis of the compressive strength.

Pressing time also influences compressive strength, though its effect is dependent on the pressing temperature. As shown in **Figure 4b**, the compressive strength generally increases with pressing time; however, the rate and extent of this increase vary with temperature. At lower temperatures (100–110 °C), a minimum pressing time of 6 min was required to achieve measurable strength, indicating a slower consolidation process. At intermediate temperatures (120–130 °C), sufficient strength was achieved with a shorter pressing duration (4 min),

indicating more efficient binder activation. However, extended pressing times beyond 10 min at 130 °C led to cracking, suggesting thermal overstress. At 140 °C, although initial strength was observed even after 2 min of pressing, further pressing resulted in structural failure. These observations suggest that while longer pressing times can enhance strength, they must be carefully optimized in conjunction with temperature to prevent thermal degradation of organic matter in the BSG matrix.

Taken together, the results underscore the importance of balancing temperature and time during hot pressing. To achieve optimal compressive performance while minimizing material damage, a pressing temperature of 120-130 °C and a duration of 10-15 min appear to be ideal for the BSG binder formulation, based on the support vector regression analysis in **Figure 4c**.

The significance of BSG consolidation in strength development is evidenced by the in situ height measurements during hot pressing. In **Figure 5a,** solid lines correspond to specimens that achieved measurable strength, whereas dashed lines indicate binder failure. Specimen height decreased progressively with pressing time, and the consolidation rate increased at higher temperatures, consistent with the reduced minimum pressing time required to attain measurable strength. Notably, the specimen pressed at 140 °C began to expand after 4 min and ultimately failed to form a binder. These results indicate that laser-based height measurements provide a reliable indicator of binder formation in BSG.



252

253 **Figure 5**. Consolidation of the BSG binders hot-pressed at 20 MPa during and after hot pressing under various
254 pressing temperatures and durations: (a) in situ specimen height changes at different temperatures, (b) correlation
255 between compressive strength and specimen height (caliper data measured after 1 day of curing; laser data
256 obtained from in situ height observation), and (c) correlation between the compressive strength and bulk density.

257

258 However, in situ consolidation alone does not fully account for variations in
259 compressive strength. **Figure 5b** illustrates the correlation between compressive strength and
260 specimen height. The dashed lines in faded colors show the in situ specimen height measured
261 by the laser sensor at the end of hot pressing (15 min). At a given temperature, compressive
262 strength generally increased with decreasing specimen height; however, distinct trends emerged
263 across different temperatures. For instance, the data for the specimens pressed at 100 °C and
264 120 °C differed from those for the specimens pressed at 110 °C and 130 °C. Therefore, the
265 laser-measurement trends do not align across all pressing temperatures.

266 In contrast, the caliper measurements obtained after 1 day of curing showed a more
267 consistent correlation with compressive strength. In **Figure 5b**, the solid lines represent the
268 specimen height measured using a caliper after the curing period. The post-curing recovery of
269 specimen height shifted the caliper data to the right relative to the laser measurements. Notably,
270 compressive strength increased significantly following this recovery, underscoring the need for
271 a 1-day curing period prior to mechanical testing. This recovery behavior resulted in a unified
272 trend up to 120 °C. However, the data at 130 °C remained deviated, likely due to temperature-
273 induced structural modifications.

Bulk density was identified as the most reliable indicator of compressive strength (**Figure 5c**). Because it incorporates both specimen height and weight, bulk density effectively explains the minor anomaly observed in the caliper data at 120 °C (dashed circles in **Figures 5b** and **5c**), which was caused by a slightly higher initial BSG mass. Moreover, the bulk density of specimens pressed at 130 °C showed a more pronounced deviation from the overall trend than the caliper-based measurements. This behavior suggests thermal degradation during hot pressing, despite the comparable compressive strengths of the specimens at 120 °C and 130 °C. As a result, a pressing temperature of 120 °C was determined to be optimal for the raw BSG within the experimental range investigated in this study.

The effect of pressing pressure on the compressive strength of the BSG binder at 120 °C for 10 min is presented in **Figure 6a**. The compressive strength increased linearly with pressure up to 20 MPa, beyond which it plateaued. The inverse trend was observed in specimen height, as shown in **Figure 6b**, suggesting that strength development is closely related to binder consolidation.

When the pressing temperature is held constant, in situ laser measurements can effectively substitute for caliper measurements. The caliper data (solid lines) and laser data (dashed lines) exhibited consistent trends, indicating that specimens subjected to different pressures underwent similar expansion after one day of curing. Although bulk density also showed a strong correlation with compressive strength (**Figure 6c**), it is impractical to determine bulk density at every pressing time of interest. Therefore, in situ laser measurements provide a practical approach for optimizing the pressure–time relationship at a given pressing temperature.

In summary, the optimal hot-pressing conditions for the raw BSG binder were a pressing temperature of 120 °C, a pressing time of 10 min, and a pressure of 20 MPa, under which the highest compressive strength was achieved while maintaining stable binder formation.

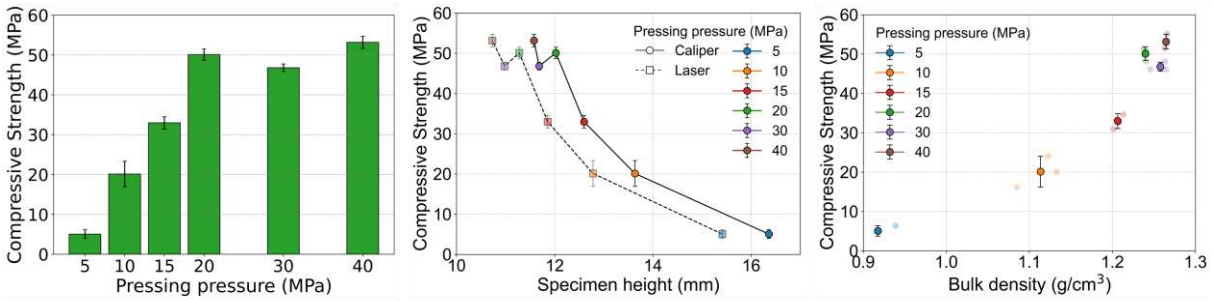


Figure 6. Effect of pressing pressure on the properties of the BSG binder hot-pressed at 120 °C for 10 min: (a) compressive strength as a function of pressure, (b) correlation between compressive strength and specimen height (caliper data measured after 1 day of curing; laser data obtained from in situ height observation), and (c) correlation between compressive strength and bulk density.

3.2 Removal of non-fibrous organic components from raw BSG

3.2.1 Factors governing binder formation failure in raw BSG

The optimal hot-pressing temperature for raw BSG was determined to be 120 °C, which is notably lower than that reported for many other fiber-based materials. For example, wood fiber composites and pelletized lignocellulosic boards typically require pressing at 180–210 °C to induce plasticization of lignin, hemicellulose, and cellulose [35]. Wheat straw fiberboards are generally processed at 160–200 °C to achieve sufficient bonding and density [36]. Similarly, the processing of natural fiber composites is limited by the thermal stability of the fibers; the tensile strength of hemp and bamboo, for instance, remains largely unchanged up to approximately 140–160 °C [37]. Since raw BSG contains similar structural polymers (lignin, hemicellulose, cellulose), a comparable optimal temperature might have been expected. However, none of the specimens pressed at 140 °C or higher achieved a compressive strength exceeding 20 MPa under any combination of pressure and pressing duration investigated in this study.

The failure of binder formation at 140 °C or higher could be closely associated with thermally induced transformations of non-fibrous organic constituents in raw BSG. Proximate analysis confirmed the presence of non-fibrous organic components, including proteins and lipids (**Table 1**), and TGA results (**Figure 7a**) also indicated the presence of pectin [38]. When raw BSG was pressed at 140 °C or higher, the pressing platen was repelled by the gas pressure inside the mold. Therefore, it was hypothesized that these organic non-fibrous components may also undergo oxidation and thermal dehydration, promoting gas evolution under heat and pressure [39]. Consequently, BSG specimens pressed at 140 °C for 6 min failed to form a consolidated binder and instead fractured transversely into two disk-shaped pieces, as shown in **Figure 7b**.

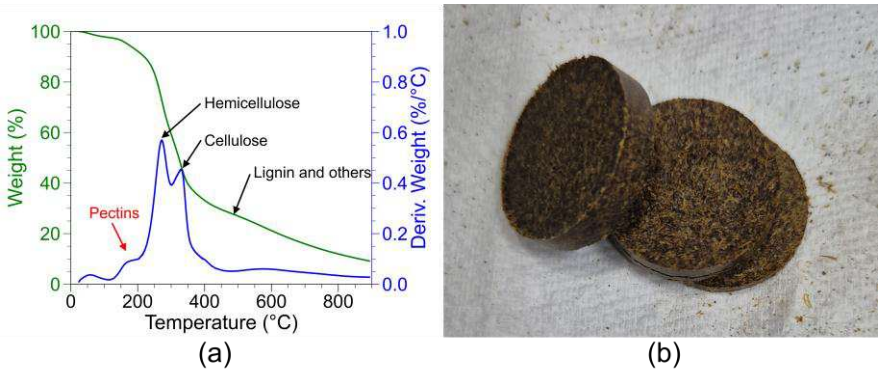


Figure 7. Non-fibrous organic components in raw BSG and the binder formation failure: (a) TGA of the raw BSG and (b) transverse fracture of the raw BSG binder pressed at 140 °C for 6 min.

These combined transformations contributed to the volumetric expansion observed in the laser measurement during pressing at 140 °C (**Figure 5a**), a behavior absent at or below 130 °C. This supports the hypothesis that the degradation of non-fibrous components generates gases or swelling forces that inhibit effective consolidation. These findings indicate that selective removal or modification of these components could suppress expansion, thereby

enhancing the compressive strength of BSG binders. Accordingly, NaOH treatment was employed to reduce the content of these interfering organic constituents in raw BSG [40-42].

3.2.2 Characteristics of BSG after NaOH treatment

The NaOH treatment applied in this study operated through two primary processes. First, exposure to the NaOH solution led to substantial dissolution of hemicellulose and lignin in the BSG binder. As shown in **Table 2** for the 0-cycle specimen, which was immersed in the NaOH solution without subsequent washing with deionized water, the hemicellulose and lignin contents decreased by approximately 85.4% and 47.4%, respectively. Instead, the cellulose content increased from 25.3% to 82%. Second, the subsequent washing process up to 15 cycles removed 35.2% of crude protein and 66.0% of crude lipids, whereas their contents remained nearly unchanged immediately after NaOH treatment (0-cycle). This indicates that crude proteins and lipids were removed primarily during the washing process rather than by the NaOH treatment itself.

Table 2. Effect of NaOH treatment on the chemical composition of BSG (wt%±Standard deviation).

	Specimens			
Components	Raw	0-cycle	7-cycles	15-cycles
Moisture	5.43 ± 0.09	2.97 ± 0.08	1.76 ± 0.10	3.17 ± 0.06
Crude protein	15.26 ± 0.07	16.02 ± 0.11	11.82 ± 0.12	10.38 ± 0.16
Crude lipid	6.20 ± 0.03	5.14 ± 0.10	1.82 ± 0.03	1.75 ± 0.04
Ash	2.24 ± 0.04	4.85 ± 0.06	3.19 ± 0.05	3.47 ± 0.04
Carbohydrate	70.86 ± 0.12	71.02 ± 0.22	81.41 ± 0.11	81.23 ± 0.18
Cellulose	12.18 ± 0.06	46.31 ± 1.62	57.22 ± 1.72	59.11 ± 2.51
Hemicellulose	22.78 ± 0.37	3.33 ± 0.81	3.85 ± 0.47	4.86 ± 0.59
Lignin	13.16 ± 1.16	6.92 ± 0.45	8.14 ± 0.16	7.56 ± 0.15

Structural changes in the BSG induced by the NaOH treatment were examined using TGA. It should be noted that residual NaOH remained in the raw BSG after treatment, as evidenced by the decrease in pH with increasing washing cycles, as shown in **Figure 8a**.

Prior to treatment, the BSG exhibited two main decomposition peaks at approximately 250 and 350 °C, corresponding to hemicellulose and cellulose, respectively [43,44]. After partial dissolution of hemicellulose and lignin by the NaOH solution, the BSG showed a single dominant peak at approximately 300 °C (**Figure 8b**). Following the washing process, this peak separated into two distinct peaks (**Figures 8c** and **8d**).

Given that 85.4% of the hemicellulose was removed by the NaOH treatment, both peaks after the treatment correspond to cellulose. Previous studies have reported that amorphous cellulose generated during grinding exhibits a lower thermal decomposition temperature [45], which can result in two peaks in the DTG curves (**Figures 8c** and **8d**).

The presence of a single cellulose peak in the 0-cycle specimen (**Figure 8b**) is therefore attributed to residual NaOH, which reduces the thermal stability of cellulose [46,47], especially by disrupting its crystalline structure [45].

The NaOH treatment effectively reduced the total organic content of the raw BSG. The residual mass at 1000 °C decreased from 17% to 5% (**Figure 8b–8d**), which supports that the thermally decomposable components were effectively removed by the NaOH solution.

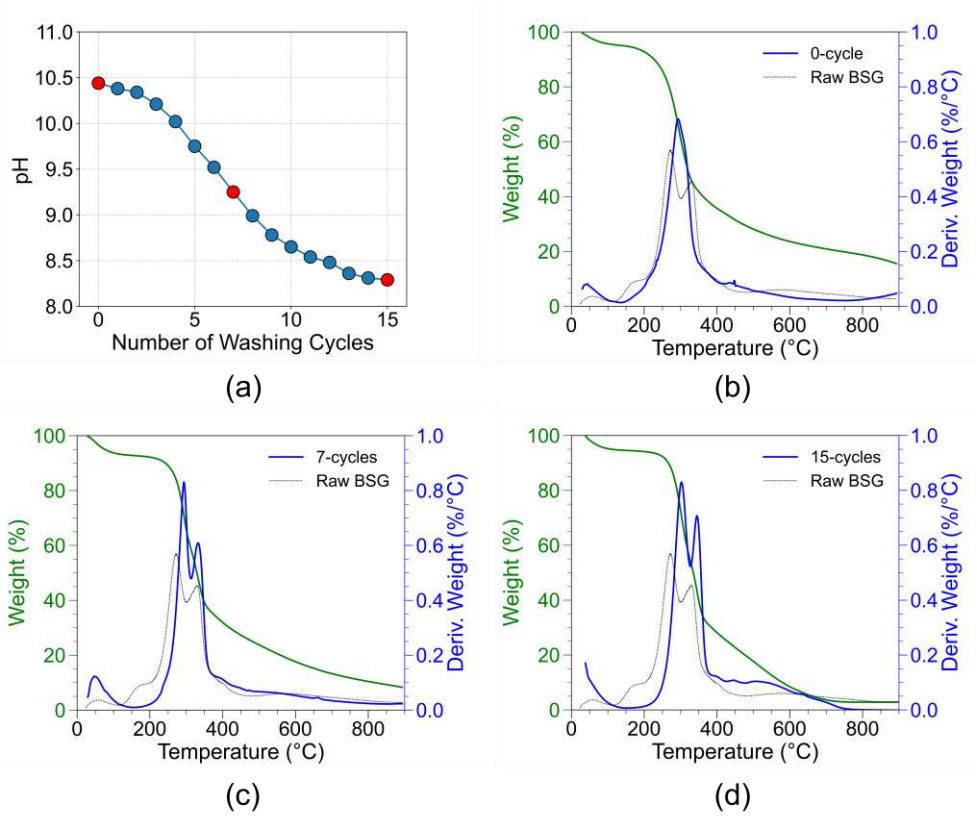


Figure 8. Effect of NaOH solution treatment on the thermal behavior of BSG: (a) variation in pH with the number of washing cycles, and TGA curves of treated BSG for (b) 0-cycle (no washing), (c) 7-cycles, and (d) 15-cycles.

The NaOH treatment successfully extended the maximum hot-pressing temperature at which a stable binder could be formed. **Figure 9a** presents the compressive strength of the NaOH-treated binder pressed at 20 MPa for 10 min. The one-sided Welch's *t*-test confirmed the significant effects of NaOH treatment on strength enhancement and washing on strength reduction, with all calculated *p*-values below 0.05, as shown in **Table 3**. The applicable temperature range for binder formation was extended to 180 °C. Since no expansion was observed from the in situ specimen height measurements, it can be inferred that the NaOH treatment suppressed expansion during hot pressing by reducing the contents of hemicellulose, crude protein, and crude lipids.

In contrast, the unwashed specimen (0 cycle) failed to form a cohesive binder at 180 °C, as evidenced by the expansion observed in in situ height measurements during hot pressing

(**Figure 9b**). This indicates that residual crude proteins and lipids hinder effective consolidation. Therefore, the removal of these organic components from raw BSG through the washing process is identified as a key factor in enhancing the compressive strength and structural integrity of the BSG binder.

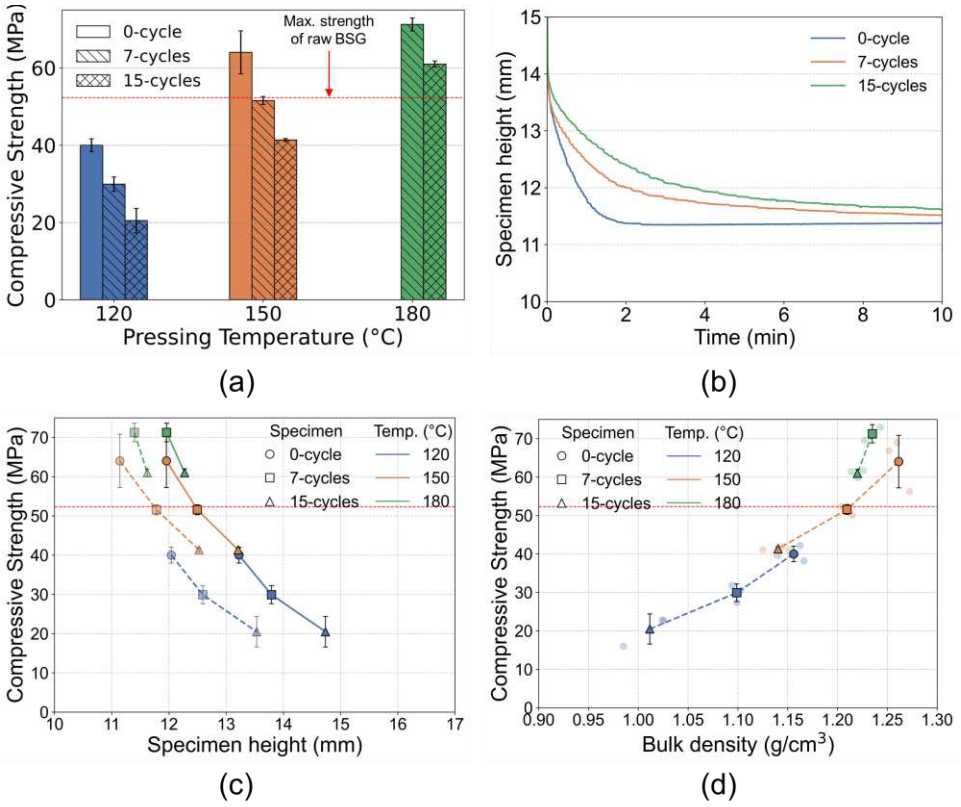


Figure 9. Effect of NaOH treatment on the compressive strength of BSG binders: (a) compressive strength results of the specimens pressed at 20 MPa for 10 min, (b) in situ specimen height changes during hot pressing at 180 °C, (c) correlation between compressive strength and specimen height (the dashed lines are caliper data measured after one day of curing; and the straight lines are laser data obtained from in situ height monitoring), and (d) correlation between compressive strength and bulk density.

Table 3. One-sided Welch's *t*-test results for the effects of NaOH treatment and washing on the compressive strength of BSG binders.

Pressing temperature (°C)	Treatment	Comparison	p-value
120	NaOH submerge	Raw vs. 0 cycle	0.0016
	Washing	0 vs. 7 cycles	0.0025
		7 vs. 15 cycles	0.0162
150	NaOH submerge	Raw vs. 0 cycle	Not applicable*
	Washing	0 vs. 7 cycles	0.0411
		7 vs. 15 cycles	0.0011
180	NaOH submerge	Raw vs. 0 cycle	Not applicable*
	Washing	0 vs. 7 cycles	Not applicable*
		7 vs. 15 cycles	0.0382

* Statistical analysis was not applicable to comparisons involving specimens for which binder formation failed.

The NaOH treatment enhanced the maximum compressive strength of the BSG binder. At a pressing temperature of 120 °C, the treated specimens exhibited lower compressive strength than the untreated raw BSG binder. However, at 180 °C, the compressive strength of all treated BSG binders exceeded that of the raw BSG. This improvement is attributed to the partial dissolution of hemicellulose and lignin in the NaOH solution, which promotes inter-fiber crosslinking during hot pressing [48-50], although a sufficiently high pressing temperature is required to activate this effect. As a result, increasing the hot-pressing temperature from 120 °C to 180 °C increased the compressive strength by 42.3%, from 50.1 MPa to 71.3 MPa. This value substantially exceeded the compressive strengths of previous fiber-based materials, which range from approximately 20 to 22 MPa [51,52].

Excessive washing after NaOH treatment reduced compressive strength. At a given hot-pressing temperature, the strength decreased nearly linearly with increasing numbers of washing cycles. However, omitting the washing step limited the applicable pressing temperature to 150 °C or lower. Previous studies have reported that NaOH treatment can enhance strength by disrupting fiber structures and promoting inter-fiber interlocking [48].

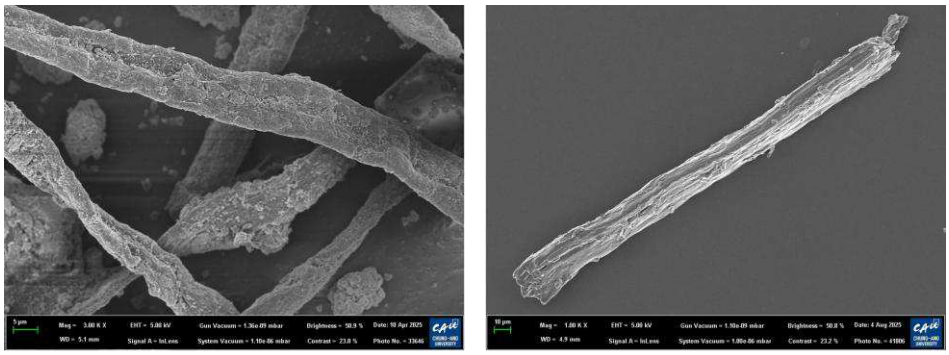
Therefore, optimization of the NaOH treatment and washing conditions is required to balance the removal of organic components with the retention of fiber reactivity.

The consolidation behavior of NaOH-treated BSG was correlated with compressive strength, as shown in **Figure 9c**. The in situ height change (dashed lines) decreased as compressive strength increased; the correlation varied with pressing temperature; and all specimens exhibited some expansion after 1 day of curing, as observed in the raw BSG binders. Similarly, bulk density demonstrated a strong correlation with compressive strength (**Figure 9d**). The data for specimens pressed at 180 °C deviated slightly from the overall trend. The lower bulk density at this temperature indicates mass loss during hot pressing, likely due to fiber decomposition. As expected, binder formation failed at 210 °C, accompanied by evidence of thermal degradation.

These results suggest that in situ specimen height measurements are valuable for optimizing pressing time and pressure under given temperature conditions, while bulk density serves as a reliable indicator of compressive strength and the onset of thermal damage in fibers.

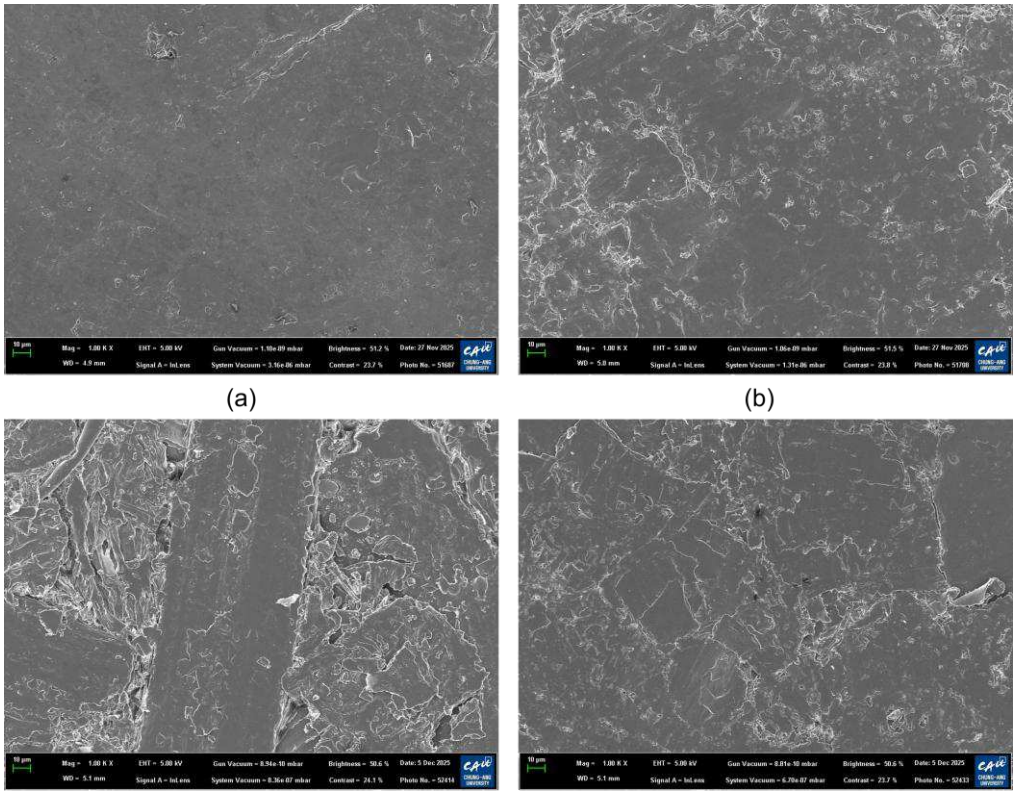
3.3. Visual observation

The effect of the NaOH solution treatment on the fiber morphology of BSG was examined using SEM. The surfaces of the raw BSG fibers were covered with adhering materials (**Figure 10a**), whereas the treated specimen of 15-cycle exhibited a relatively clean and well-defined fiber morphology (**Figure 10b**). Morphological changes in the BSG binder surface were observed, as shown in **Figure 11**. The raw BSG binder exhibited a relatively smooth surface, whereas the treated specimens developed a rougher morphology following NaOH treatment and subsequent washing. These morphological changes demonstrate the removal of non-fibrous organics, which enhanced inter-fiber interactions and facilitated improved crosslinking during hot pressing, eventually resulting in higher compressive strength.



(a) (b)

Figure 10. SEM images of BSG fibers: (a) raw and (b) 15-cycles



(a) (b)

(c) (d)

Figure 11. SEM images of the BSG binders pressed for 10 min under 20 MPa. The raw BSG binder was pressed at 120 °C, whereas the treated specimens were pressed at 150 °C: (a) raw, (b) 0-cycle, (c) 7-cycles, and (d) 15-cycles.

The optical observations in **Figure 12** provide insight into the nature of the adhesive materials surrounding the raw BSG fibers. When the raw BSG was hot-pressed at 120 °C, the fibers appeared darkened, indicating thermal degradation of these adhesive components. At temperatures above 120 °C, these materials likely generated gases during hot pressing, leading

to failure in binder formation. In contrast, after NaOH treatment, the specimens exhibited a uniform surface color with no visible signs of thermal degradation, suggesting that these reactive components had been removed. Overall, the NaOH solution treatment plays a critical role in enabling stable BSG binder formation during hot pressing.

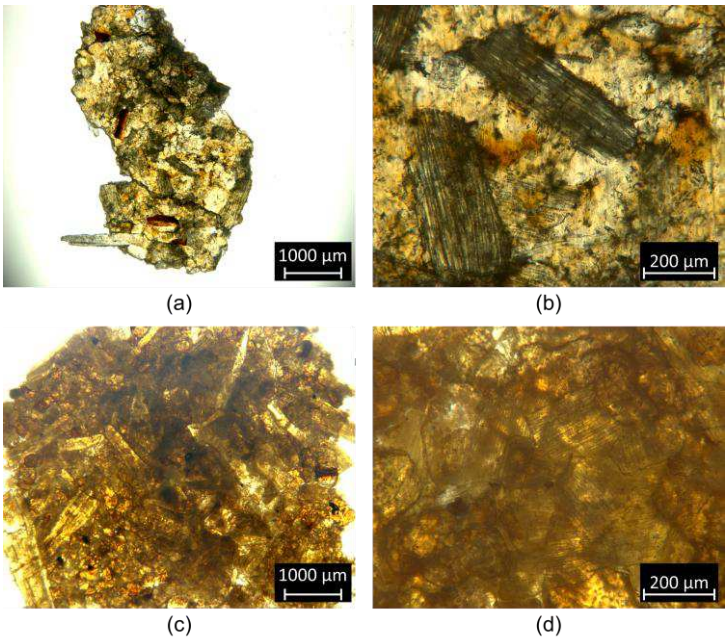


Figure 12. Optical microscopy images of the BSG binder pressed for 10 min under 20 MPa: (a, b) raw BSG binder pressed at 120 °C; (c, d) 15-cycle BSG binder pressed at 150 °C.

3.4. Correlation between the compressive strength and the flexural strength

The compressive strength of the BSG binder can serve as an effective indicator of its flexural strength. Since many hot-pressed binders are intended for board-type applications, their mechanical performance is often evaluated by flexural strength. As shown in **Figure 13**, compressive strength exhibited a trend consistent with flexural strength, with both properties increasing concurrently.

Flexural strength appeared to be more sensitive to thermal damage in BSG fibers. For example, in the raw BSG binder pressed at 130 °C, flexural strength decreased while compressive strength continued to increase. Despite this discrepancy, the overall correlation between the two properties suggests that optimizing hot-pressing conditions based on

compressive strength is a reasonable approach, offering the additional advantage of reduced material consumption.

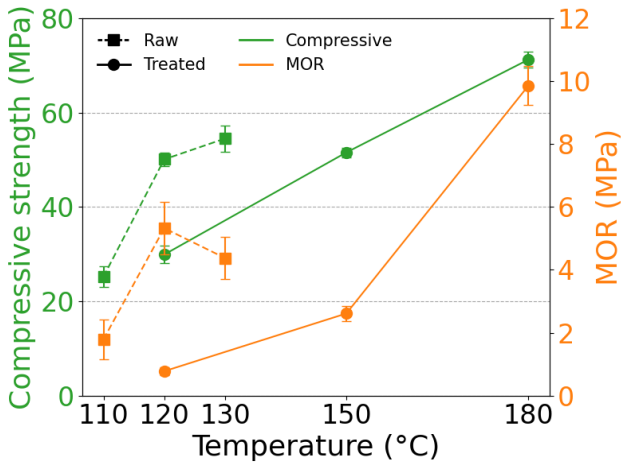


Figure 13. Relationship between compressive strength and flexural strength of the BSG binder.

4. Conclusion

This study investigated the influence of NaOH pretreatment on the hot-pressing response of brewer's spent grain (BSG) and the resulting properties of binderless fiber material. Building on earlier demonstrations of BSG-only particleboards, the present work specifically examined in situ consolidation, pressing-induced expansion, and the effects of compositional modification on the processing-temperature range. The principal findings are summarized below:

1. For untreated BSG, compressive strength was closely related to consolidation and bulk density. A strength of 50.1 MPa was obtained at 120 °C, 20 MPa, and 10 min under the selected processing conditions. At higher temperatures, pressing-induced expansion and cracking restricted stable composite formation.
2. In situ laser measurements resolved the evolution of specimen height during hot pressing and revealed the onset of expansion in conditions associated with unsuccessful consolidation. Height measurements provided useful within-temperature indicators of pressing behavior, whereas bulk density showed a more

consistent relationship with final compressive strength across different temperatures. The observed expansion is consistent with thermally induced volatile release or other swelling processes, although the evolved gases were not directly identified.

3. Treatment with 0.1 M NaOH markedly altered BSG composition, reducing the measured hemicellulose and lignin fractions by approximately 85.4% and 47.4%, respectively. Subsequent washing further lowered crude protein and lipid contents. The combined treatment enabled stable hot pressing up to 180 °C within the investigated conditions, whereas untreated BSG showed severe deterioration at substantially lower temperatures. These results associate compositional modification with improved high-temperature pressing stability, without establishing a unique chemical bonding mechanism.
4. The maximum compressive strength of the treated composite was 71.3 MPa, approximately 32% higher than the maximum recorded for untreated BSG (about 54 MPa). However, treatment did not improve strength at every temperature: at 120 °C, the treated material was weaker than untreated BSG. Washing also produced a trade-off between removal of residual constituents and strength retention, emphasizing the need to optimize pretreatment and rinsing together with pressing conditions.

Overall, the findings extend prior BSG-only binderless-board research by linking alkali pretreatment to real-time consolidation behavior and the attainable pressing-temperature range. Before practical application, further work is needed to establish water resistance, dimensional stability, biological durability, and performance at larger panel scales. Direct analysis of evolved gases and bonding chemistry would also help test the proposed mechanisms. Finally,

the environmental implications of NaOH use, repeated washing, and drying should be quantified before claims of improved sustainability are made.

Acknowledgments

Data availability statement

All data generated or analyzed during this study are included in this published article. Please contact Prof. S. Park in case of any queries regarding this study.

Author contributions

Sungwoo Park*: Conceptualization, Funding acquisition, Supervision, Writing – original draft, Writing – review & editing; Seongjong Kim: Data curation, Formal analysis, Visualization; Choongwan Koo: Validation, Writing – review & editing; Yang-Ju Son: Validation, Writing – review & editing

Funding

This work was supported by the National Research Foundation of Korea (NRF) grant funded by the Korean government (MSIT) (No. RS-2023-00217322 and RS-2025-00521537).

Competing interests

The authors declare no competing interests.

References

1 Calisto Friant, M., Vermeulen, W. J. V. & Salomone, R. Analysing European Union circular economy policies: words versus actions. *Sustainable Production and Consumption* **27**, 337–353 (2021). https://doi.org/10.1016/j.spc.2020.11.001

2 Nigam, P. S. An overview: Recycling of solid barley waste generated as a by-product in distillery and brewery. *Waste management* **62**, 255–261 (2017).

3 Lynch, K. M., Steffen, E. J. & Arendt, E. K. Brewers' spent grain: a review with an emphasis on food and health. *Journal of the Institute of Brewing* **122**, 553–568 (2016).

4 Swart, L. J., Bedzo, O. K., van Rensburg, E. & Görgens, J. F. Pilot-scale xylooligosaccharide production through steam explosion of screw press–dried brewers' spent grains. *Biomass Conversion and Biorefinery* **12**, 1295–1309 (2022).

5 Capossio, J. P. *et al.* Sustainable solar drying of brewer's spent grains: a comparison with conventional electric convective drying. *Processes* **10**, 339 (2022).

6 Qazanfarzadeh, Z., Ganesan, A. R., Mariniello, L., Conterno, L. & Kumaravel, V. Valorization of brewer's spent grain for sustainable food packaging. *Journal of Cleaner Production* **385**, 135726 (2023).

7 Agrawal, D., Gopaliya, D., Willoughby, N., Khare, S. K. & Kumar, V. Recycling potential of brewer's spent grains for circular biorefineries. *Current Opinion in Green and Sustainable Chemistry* **40**, 100748 (2023).

8 Mussatto, S. I., Dragone, G. & Roberto, I. C. Brewers' spent grain: generation, characteristics and potential applications. *Journal of Cereal Science* **43**, 1–14 (2006). https://doi.org/10.1016/j.jcs.2005.06.001

9 Mussatto, S. I. & Roberto, I. C. Acid hydrolysis and fermentation of brewer's spent grain to produce xylitol. *Journal of the Science of Food and Agriculture* **85**, 2453–2460 (2005). https://doi.org/10.1002/jsfa.2276

10 Jackowski, M., Niedzwiecki, L., Jagiello, K., Uchanska, O. & Trusek, A. Brewer's Spent Grains-Valuable Beer Industry By-Product. *Biomolecules* **10** (2020). https://doi.org/10.3390/biom10121669

11 Kerby, C. & Vriesekoop, F. An Overview of the Utilisation of Brewery By-Products as Generated by British Craft Breweries. *Beverages* **3** (2017). https://doi.org/10.3390/beverages3020024

12 Russ, W., Mörtel, H. & Meyer-Pittroff, R. Application of spent grains to increase porosity in bricks. *Construction and Building Materials* **19**, 117–126 (2005). https://doi.org/10.1016/j.conbuildmat.2004.05.014

13 Ferraz, E. *et al.* Spent Brewery Grains for Improvement of Thermal Insulation of Ceramic Bricks. *Journal of Materials in Civil Engineering* **25**, 1638–1646 (2013). https://doi.org/10.1061/(asce)mt.1943-5533.0000729

14 Sheets, J. P., Yang, L., Ge, X., Wang, Z. & Li, Y. Beyond land application: Emerging technologies for the treatment and reuse of anaerobically digested agricultural and food waste. *Waste Manag* **44**, 94–115 (2015). https://doi.org/10.1016/j.wasman.2015.07.037

15 Barbu, M. C. *et al.* Potential of Brewer's Spent Grain as a Potential Replacement of Wood in pMDI, UF or MUF Bonded Particleboard. *Polymers (Basel)* **13** (2021). https://doi.org/10.3390/polym13030319

16 Aguillón, B. *et al.* Sorbitol glycidyl ether Epoxy/Brewer's spent grain biocomposite for fiberboard applications. *Case Studies in Chemical and Environmental Engineering* **9** (2024). https://doi.org/10.1016/j.cscee.2024.100705

17 Klímek, P., Wimmer, R., Kumar Mishra, P. & Kúdela, J. Utilizing brewer's-spent-grain in wood-based particleboard manufacturing. *Journal of Cleaner Production* **141**, 812–817 (2017). https://doi.org/10.1016/j.jclepro.2016.09.152

18 Nehra, A., Biswas, D. & Roy, S. Fabrication of brewer’s spent grain fortified bio-based edible bowls: a promising alternative to plastic containers. *Biomass Conversion and Biorefinery* **14**, 16425–16434 (2022). https://doi.org/10.1007/s13399-022-03698-1

19 Börcsök, Z. & Pásztory, Z. The role of lignin in wood working processes using elevated temperatures: an abbreviated literature survey. *European Journal of Wood and Wood Products* **79**, 511–526 (2020). https://doi.org/10.1007/s00107-020-01637-3

20 Bouajila, J., Limare, A., Joly, C. & Dole, P. Lignin plasticization to improve binderless fiberboard mechanical properties. *Polymer Engineering & Science* **45**, 809–816 (2005). https://doi.org/10.1002/pen.20342

21 Widyorini, R., Xu, J., Watanabe, T. & Kawai, S. Chemical changes in steam-pressed kenaf core binderless particleboard. *Journal of Wood Science* **51**, 26–32 (2005). https://doi.org/10.1007/s10086-003-0608-9

22 Okuda, N., Hori, K. & Sato, M. Chemical changes of kenaf core binderless boards during hot pressing (I): influence of the pressing temperature condition. *Journal of Wood Science* **52**, 244–248 (2006). https://doi.org/10.1007/s10086-005-0761-4

23 Pintiaux, T., Viet, D., Vandenbossche, V., Rigal, L. & Rouilly, A. Binderless Materials Obtained by Thermo-Compressive Processing of Lignocellulosic Fibers: A Comprehensive Review. *BioResources* **10** (2015).

24 Nasir, M. *et al.* Recent development in binderless fiber-board fabrication from agricultural residues: A review. *Construction and Building Materials* **211**, 502–516 (2019). https://doi.org/10.1016/j.conbuildmat.2019.03.279

25 Hashim, R. *et al.* Characterization of raw materials and manufactured binderless particleboard from oil palm biomass. *Materials & Design* **32**, 246–254 (2011). https://doi.org/10.1016/j.matdes.2010.05.059

26 Xia, Z. & Xu, J.-y. in *2010 International Conference on Mechanic Automation and Control Engineering.* 5366–5368 (IEEE).

27 Arauzo, P. J., Olszewski, M. P. & Kruse, A. Hydrothermal Carbonization Brewer's Spent Grains with the Focus on Improving the Degradation of the Feedstock. *Energies* **11** (2018). https://doi.org/10.3390/en11113226

28 Kurokochi, Y. & Sato, M. Properties of binderless board made from rice straw: The morphological effect of particles. *Industrial Crops and Products* **69**, 55–59 (2015). https://doi.org/10.1016/j.indcrop.2015.01.044

29 van Dam, J. E. G., van den Oever, M. J. A. & Keijsers, E. R. P. Production process for high density high performance binderless boards from whole coconut husk. *Industrial Crops and Products* **20**, 97–101 (2004). https://doi.org/10.1016/j.indcrop.2003.12.017

30 Suzuki, S. *et al.* Preparation of Binderless Boards from Steam Exploded Pulps of Oil Palm(Elaeis guneensisJaxq.) Fronds and Structural Characteristics of Lignin and Wall Polysaccharides in Steam Exploded Pulps to be Discussed for Self-Bindings. *Holzforschung* **52**, 417–426 (1998). https://doi.org/10.1515/hfsg.1998.52.4.417

31 Rossi, L. *et al.* Sustainable Particleboards Based on Brewer's Spent Grains. *Polymers (Basel)* **16** (2023). https://doi.org/10.3390/polym16010059

32 AACC. *Approved Methods of Analysis, tenth ed.*, (AACC International, 2000).

643 33 Jung, S.-J., Kim, S.-H. & Chung, I.-M. Comparison of lignin, cellulose, and hemicellulose
644 contents for biofuels utilization among 4 types of lignocellulosic crops. *Biomass and*
645 *Bioenergy* **83**, 322–327 (2015). https://doi.org/10.1016/j.biombioe.2015.10.007

646 34 Qin, F., Johansen, A. Z. & Mussatto, S. I. Evaluation of different pretreatment strategies
647 for protein extraction from brewer's spent grains. *Industrial Crops and Products* **125**, 443–
648 453 (2018). https://doi.org/10.1016/j.indcrop.2018.09.017

649 35 Börcsök, Z. & Pásztory, Z. The role of lignin in wood working processes using elevated
650 temperatures: an abbreviated literature survey. *European Journal of Wood and Wood*
651 *Products* **79**, 511–526 (2021).

652 36 Valchev, I., Savov, V., Yordanov, I., Petrin, S. & Antov, P. Effect of Hot-Pressing
653 Temperature on the Properties of Eco-Friendly Fiberboard Panels Bonded with Hydrolysis
654 Lignin and Phenol-Formaldehyde Resin. *Polymers (Basel)* **16** (2024).
655 https://doi.org/10.3390/polym16081059

656 37 Elfaleh, I. *et al.* A comprehensive review of natural fibers and their composites: An eco-
657 friendly alternative to conventional materials. *Results in Engineering* **19** (2023).
658 https://doi.org/10.1016/j.rineng.2023.101271

659 38 Gomez-Hernandez, E. *et al.* High-Energy Milling as a Pre-Treatment Alternative for
660 Lignocellulosic Fibers Derived from Brewer's Spent Grain. *Polymers (Basel)* **17** (2025).
661 https://doi.org/10.3390/polym17091156

662 39 Naibaho, J., Pudlo, A., Korzeniowska, M., Lu, Y. & Yang, B. Alteration of volatile
663 compounds profile of brewers' spent grain by bath-ultrasonication and its combination with
664 conventional water-bath and autoclave treatment. *Ultrason Sonochem* **90**, 106192 (2022).
665 https://doi.org/10.1016/j.ultsonch.2022.106192

666 40 Mishra, P. K., Gregor, T. & Wimmer, R. Utilising Brewer's Spent Grain as a Source of
667 Cellulose Nanofibres Following Separation of Protein-based Biomass. *BioResources* **12**
668 (2016). https://doi.org/10.15376/biores.12.1.107-116

669 41 da Fonseca, Y. A., Gurgel, L. V. A., Baêta, B. E. L., Dragone, G. & Mussatto, S. I. Reduced-
670 pressure alkaline pretreatment as an innovative and sustainable technology to extract
671 protein from brewer's spent grain. *Journal of Cleaner Production* **416** (2023).
672 https://doi.org/10.1016/j.jclepro.2023.137966

673 42 Morales-Juarez, A. A., Terrazas Armendariz, L. D., Alcocer-Gonzalez, J. M. & Chavez-
674 Guerrero, L. Potential of Nanocellulose as a Dietary Fiber Isolated from Brewer's Spent
675 Grain. *Polymers (Basel)* **15** (2023). https://doi.org/10.3390/polym15173613

676 43 Yang, H. *et al.* In-Depth Investigation of Biomass Pyrolysis Based on Three Major
677 Components: Hemicellulose, Cellulose and Lignin. *Energy & Fuels* **20**, 388–393 (2005).
678 https://doi.org/10.1021/ef0580117

679 44 Yang, H., Yan, R., Chen, H., Lee, D. H. & Zheng, C. Characteristics of hemicellulose,
680 cellulose and lignin pyrolysis. *Fuel* **86**, 1781–1788 (2007).
681 https://doi.org/10.1016/j.fuel.2006.12.013

45 Wang, Z. *et al.* Effect of cellulose crystallinity on the formation of a liquid intermediate and on product distribution during pyrolysis. *Journal of Analytical and Applied Pyrolysis* **100**, 56–66 (2013). https://doi.org/10.1016/j.jaap.2012.11.017

46 Wang, M., Zhang, S., Liu, X., Ma, Y. & Wang, J. Catalytic co-pyrolysis of cellulose over alkali and alkaline earth metal salts for levoglucosan production. *Industrial Crops and Products* **201** (2023). https://doi.org/10.1016/j.indcrop.2023.116925

47 Wang, W., Lemaire, R., Bensakhria, A. & Luart, D. Thermogravimetric Analysis and Kinetic Modeling of the AAEM-Catalyzed Pyrolysis of Woody Biomass. *Molecules* **27** (2022). https://doi.org/10.3390/molecules27227662

48 Song, J. *et al.* Processing bulk natural wood into a high-performance structural material. *Nature* **554**, 224–228 (2018). https://doi.org/10.1038/nature25476

49 Huang, W. *et al.* Fabrication of High-Performance Densified Wood via High-Pressure Steam Treatment and Hot-Pressing. *Polymers (Basel)* **16** (2024). https://doi.org/10.3390/polym16070939

50 Xiao, L., Ding, Y. & Yan, G. Effect of hot-pressing temperature on characteristics of alkali pretreated reed straw bio-board. *Journal of Wood Chemistry and Technology* **41**, 160–168 (2021). https://doi.org/10.1080/02773813.2021.1949351

51 Lang, S. *et al.* Research on the hot densification mechanism of biomass wastes based on molecular dynamics simulation and components adjustment method. *Energy* **294** (2024). https://doi.org/10.1016/j.energy.2024.130902

52 Mirindi, D., Onchiri, R. O. & Thuo, J. Physico-Mechanical Properties of Particleboards Produced from Macadamia Nutshell and Gum Arabic. *Applied Sciences* **11** (2021). https://doi.org/10.3390/app112311138

Legends

Table 1. Chemical composition of raw BSG.

Table 2. Effect of NaOH treatment on the chemical composition of BSG (wt%±Standard deviation).

Table 3. One-sided Welch's *t*-test results for the effects of NaOH treatment and washing on the compressive strength of BSG binders.

Figure 1. Sieve-based particle size distribution of the prepared BSG powder.

Figure 2. Schematic drawing of the hot-pressing machine and the molds used in this study.

Figure 3. Example of in situ specimen height measurement during BSG binder formation, hot-pressed at 130 °C under 20 MPa pressure for 15 min using a laser displacement sensor.

Figure 4. Compressive strength of BSG binders hot-pressed under a constant pressure at 20 MPa: (a) compressive strength at varying temperatures with different pressing times, (b) strength development over time at different temperatures, and (c) support vector regression analysis of the compressive strength.

Figure 5. Consolidation of the BSG binders hot-pressed at 20 MPa during and after hot pressing under various pressing temperatures and durations: (a) in situ specimen height changes at different temperatures, (b) correlation between compressive strength and specimen height (caliper data measured after 1 day of curing; laser data obtained from in situ height observation), and (c) correlation between the compressive strength and bulk density.

Figure 6. Effect of pressing pressure on the properties of the BSG binder hot-pressed at 120 °C for 10 min: (a) compressive strength as a function of pressure, (b) correlation between compressive strength and specimen height (caliper data measured after 1 day of curing; laser data obtained from in situ height observation), and (c) correlation between compressive strength and bulk density.

Figure 7. Non-fibrous organic components in raw BSG and the binder formation failure: (a) TGA of the raw BSG and (b) transverse fracture of the raw BSG binder pressed at 140 °C for 6 min.

Figure 8. Effect of NaOH solution treatment on the thermal behavior of BSG: (a) variation in pH with the number of washing cycles, and TGA curves of treated BSG for (b) 0-cycle (no washing), (c) 7-cycles, and (d) 15-cycles.

Figure 9. Effect of NaOH treatment on the compressive strength of BSG binders: (a) compressive strength results of the specimens pressed at 20 MPa for 10 min, (b) in situ specimen height changes during hot pressing at 180 °C, (c) correlation between compressive strength and specimen height (the dashed lines are caliper data measured after one day of curing; and the straight lines are laser data

obtained from in situ height monitoring), and (d) correlation between compressive strength and bulk density.

Figure 10. SEM images of BSG fibers: (a) raw and (b) 15-cycles

Figure 11. SEM images of the BSG binders pressed for 10 min under 20 MPa. The raw BSG binder was pressed at 120 °C, whereas the treated specimens were pressed at 150 °C: (a) raw, (b) 0-cycle, (c) 7-cycles, and (d) 15-cycles.

Figure 12. Optical microscopy images of the BSG binder pressed for 10 min under 20 MPa: (a, b) raw BSG binder pressed at 120 °C; (c, d) 15-cycle BSG binder pressed at 150 °C.

Figure 13. Relationship between compressive strength and flexural strength of the BSG binder.